

The Synthetic Heteroarotinoid SHetA2 Induces Apoptosis in Squamous Carcinoma Cells through a Receptor-independent and Mitochondria-dependent Pathway¹

Kyung-Hee Chun, Doris M. Benbrook, K. Darrell Berlin, Waun Ki Hong, and Reuben Lotan²

Department of Thoracic/Head and Neck Medical Oncology, The University of Texas M. D. Anderson Cancer Center, Houston, Texas 77030 [K.-H. C., W. K. H., R. L.]; Department of Obstetrics and Gynecology, and Department of Biochemistry and Molecular Biology, The University of Oklahoma Health Sciences Center, Oklahoma City, Oklahoma 73190 [D. M. B.]; and The Department of Chemistry, Oklahoma State University, Stillwater, Oklahoma 74078 [K. D. B.]

ABSTRACT

Retinoids that regulate cell growth, differentiation, and apoptosis have shown promising results in preclinical studies and in a few clinical trials of cancer chemoprevention and therapy. However, the clinical use of retinoids is limited by resistance of certain malignant cells to their antitumor effects and by side effects. To identify more potent retinoids, we examined the effects of heteroarotinoids (Hets), new synthetic retinoids with reduced toxicity, on the growth of human head and neck squamous cell carcinoma (HNSCC) lines. Six Hets with different retinoic acid receptor activation potentials were found to exhibit distinct efficacies. The most potent among the Hets examined, SHetA2, {[4-(nitrophenyl)amino][2,2,4,4-tetramethyl thiochroman-6-yl)amino] methane-1-thione}, was more effective than either all-*trans*- or 9-*cis*-RA. The growth of UMSCC38, the most sensitive among the eight HNSCC cell lines examined, was suppressed by SHetA2 in a dose- and time-dependent fashion. SHetA2-induced apoptosis in UMSCC38 cells was comparable with *N*-(4-hydroxyphenyl)retinamide (4HPR). Reactive oxygen species (ROS) generation in the UMSCC38 cells was increased by SHetA2, and this effect was suppressed by the antioxidant butylated hydroxyanisole, which also suppressed SHetA2-induced apoptosis. SHetA2 suppressed mitochondrial permeability transition and enhanced cytochrome *c* release from mitochondria. Both of these effects were prevented by cyclosporin A, which also decreased SHetA2-induced apoptosis. SHetA2 increased caspase-3-like activity, and a caspase-3 inhibitor diminished SHetA2-induced apoptosis. Several retinoid receptor antagonists failed to prevent apoptosis induction by SHetA2. These results demonstrate that SHetA2 is a potent, receptor-independent, apoptosis inducer that acts on the mitochondria in HNSCC cells. Further investigation of the potential of SHetA2 in prevention and therapy of HNSCC is warranted also because of much lower toxicities compared with receptor active retinoids.

INTRODUCTION

Retinoids, natural and synthetic vitamin A analogues, have demonstrated potential in the chemoprevention of a variety of cancers in animal models (1) and in humans at increased risk for developing primary or second primary cancers (2–4). Certain retinoids can also inhibit the growth, induce the differentiation, or enhance apoptosis of fully malignant cells *in vitro* (5) and *in vivo* (6–8). Head and neck premalignant and malignant cells are susceptible to retinoid chemopreventive (2, 3) and therapeutic (7–9) effects *in vivo*. Studies with cultured HNSCCs³ have demonstrated that retinoids can suppress cell

proliferation, inhibit the formation of colonies in semisolid agarose, and decrease the growth of HNSCC multicellular spheroids (10, 11). In addition, retinoids suppress the expression of several squamous differentiation markers and inhibit cornified envelope formation (10, 12).

Many HNSCC cell lines exhibit relative resistance to the growth-inhibitory effects of ATRA and 9-*cis*-RA, although some synthetic analogues are quite potent (13). For example, 4HPR is an effective inducer of apoptosis, albeit at high (>3 μM) concentrations (14).

The clinical application of ATRA is limited by a number of side effects (2). Likewise, 4HPR has a significant side effect (night blindness) resulting mainly from reduction in circulating retinol levels (15). Therefore, new retinoids are being synthesized and characterized with the hope of improving their antitumor and chemopreventive efficacy. The toxicity and teratogenicity of retinoids are associated with the activation of nuclear RARs and RXRs that act as transcription factors (16–18). Thus retinoid-related molecules, which inhibit the growth of cancer cells or induce apoptosis by receptor-independent molecules, may be devoid of side effects.

Certain retinoids belonging to the class of Hets have demonstrated anticancer activity as well as low toxicity (19–22). Hets have demonstrated growth-inhibitory activity against carcinoma cell lines derived from cervix, vulva, ovary, and HNSCC tumors (20). Some Hets caused a reduction in tumor size in a xenograft model of human HNSCC cell line UMSCC38 in nude mice (21). Recently, some receptor-activating and receptor-independent Hets were found to induce differentiation and apoptosis in organotypic cultures of ovarian carcinoma (22). Although this indicates that receptor activation is not required for apoptosis, the mechanism(s) that underlie the induction of apoptosis in cancer cells by Hets has not been investigated.

In the present study, we demonstrate the ability of some Hets to induce apoptosis in HNSCC cell lines, and we shed light on some aspects of the mechanism of apoptosis induction. Specifically, we show that the induction of apoptosis is independent of retinoid receptor signaling pathway and that it involves changes in mitochondrial permeability transition and cytochrome *c* release followed by activation of caspases 3.

MATERIALS AND METHODS

Retinoids. The Hets were synthesized as published (19, 21).⁴ SHet50 is a receptor pan-agonist, Ohet72 is specific for the RXRs, whereas SHetA2, SHetA3, and SHetA4 do not activate any of the receptors when used at doses up to 10 μM (Fig. 1). ATRA was obtained from Dr. Werner Bollag (F. Hoffmann-La Roche, Basel, Switzerland). AGN 193109 [a RAR- α , - β , and - γ antagonist (23)], was obtained from Dr. R. Chandraratna (Allergan, Irvine, CA). LG100754, a RXR antagonist (24), was obtained from Dr. R. Heyman

reactive oxygen species; RXR, retinoid X receptor; SRB, sulforhodamine B; TFP, trifluoperazine; TUNEL, terminal deoxynucleotidyl transferase-mediated dUTP nick-end labeling; 4HPR, *N*-(4-hydroxyphenyl)retinamide; MPTP, mitochondrial permeability transition pore; PBST, PBS and Tween 20; CsA, cyclosporin A.

⁴ S. Liu, C.W. Brown, K. D. Berlin, A. Dhar, S. Guruswamy, D. Brown, and D. M. Benbrook. Synthesis and biological evaluation of sulfur-containing Hets possessing thio- or urea moieties as three atom “linker” groups—discrimination between malignant and benign cells, submitted for publication.

Received 9/16/02; accepted 4/28/03.

The costs of publication of this article were defrayed in part by the payment of page charges. This article must therefore be hereby marked *advertisement* in accordance with 18 U.S.C. Section 1734 solely to indicate this fact.

¹ Supported in part by USPHS Grants P50-CA97007-01 Head and Neck SPORE from the National Cancer Institute, P50 DE11906 Grant from the National Institute of Dental and Craniofacial Research and by the Tobacco Settlement Funds as appropriated by the Texas State Legislature.

² To whom requests for reprints should be addressed, at Department of Thoracic/Head and Neck Medical Oncology-Box 432. The University of Texas M. D. Anderson Cancer Center, 1515 Holcombe Blvd., Houston, Texas 77030. Phone: (713) 792-8467; Fax: (713) 745-5656; E-mail: rlotan@mdanderson.org.

³ The abbreviations used are: RA, retinoic acid; ATRA, all-*trans*-RA; BHA, butylated hydroxyanisole; DCF-DA, 5,6-carboxy-2',7'-dichlorofluorescein diacetate; DiOC₆, 3,3'-dihydroxycarbocyanine iodide; Het, heteroarotinoid; HNSCC, head and neck squamous cell carcinoma; MPT, membrane permeability transition; RAR, RA receptor; ROS,

Retinoid	Structure	Receptor activation (EC50, nM) ^a					
		RAR α	RAR β	RAR γ	RXR α	RXR β	RXR γ
ATRA		350	80	10	900	1400	1100
9- <i>cis</i> -RA		191	50	45	100	200	140
4HPR		>20,000	>20,000	5,000	>20,000	ND	ND
SHetA2		No transactivation at 10,000					
SHetA3		No transactivation at 10,000					
SHetA4		No transactivation at 10,000					
SHet50		225	1004	152	84	68	302
SHetA19		No transactivation at 10,000					
OHet72		>10,000	>10,000	>10,000	294	1897	42
AGN193109		RAR antagonist ^b 2 2 3 >10,000 >10,000 >10,000					
LG100754		RXRs antagonist ^b >1000 >1000 >1000 3.4 10 9.7					

Fig. 1. Structure of the retinoids used in this study. ^a Analyzed by transcriptional activation of reporter constructs in cells transfected with individual receptors (19–22) or ^b binding to receptors (23, 24).

(Ligand Pharmaceuticals, Inc., San Diego, CA). The chemical structures and receptor selectivity of these retinoids are presented in Fig. 1.

Cell Lines and Cell Culture. Human HNSCC cell lines UMSCC17A, UMSCC17B, UMSCC22B, and UMSCC38 cell lines were obtained from Dr. T. Carey (University of Michigan, Ann Arbor, MI). HNSCC cell lines MDA886Ln, 1186, and 1483 were provided by Dr. P. G. Sacks (New York University College of Dentistry, New York, NY). SqCC/Y1 cells were provided by Dr. M. Reiss (Yale University, New Haven, CT). These cells were grown in monolayer culture in a 1:1 (v/v) mixture of DMEM and Ham's F12 medium, supplemented with 5% fetal bovine serum and antibiotics at 37°C in a humidified atmosphere consisting of 95% air and 5% CO₂.

Treatment with Hets and Determination of Cell Survival. Cells were seeded at a density of 3000 cells/well in 96-well tissue culture plates. After 24 h, cells were treated with different concentrations of retinoids. Control cultures received the same amount of DMSO (final concentrations, 0.01–0.1%) as did the treated cultures. Cell numbers were estimated on days 1, 2, and 3 by using the SRB assay as described in detail previously (13). The percentage of growth inhibition was calculated by using the equation: % growth inhibition = $(1 - At/Ac) \times 100$, where *At* and *Ac* represent the absorbance in treated and control cultures, respectively. IC₅₀, the drug concentration causing a 50% cell growth inhibition, was determined by interpolation of the dose-response curve.

Detection of Apoptosis. Cells were plated on 10-cm-diameter dishes, and, after 24 h, they received either DMSO or retinoids dissolved in DMSO. After 1, 2, and 3 days of treatment, cells were harvested by a brief trypsinization and were counted. APO-Direct TUNEL kit (Phoenix Flow Systems, Inc., San Diego, CA) was used following the manufacturer's protocol to label DNA fragments with 3'-hydroxyl ends. In addition, Annexin V-FITC Apoptosis

Detection kit (Oncogene Research Products, Cambridge, MA) was also used following the manufacturer's protocol to label externalized phosphatidylserine. Flow cytometric analysis was conducted using a Coulter EPICS Profile II flow cytometer (Coulter Corp., Miami, FL) equipped with a 488-nm argon laser. Approximately 10,000 events (cells) were evaluated for each sample. Gating of control nonapoptotic populations (cells treated with DMSO) was used as a reference to compare with treatments with retinoids. An internal control, (HL-60 cells treated with camptothecin to induce apoptosis) provided in the apoptosis detection kit, was also used to ensure that the TUNEL reaction was occurring during the staining procedure.

Assay of Generation of ROS. The net intracellular generation of ROS was measured by using the oxidation-sensitive fluorescent dye DCF-DA (Molecular Probe, Eugene, OR) as described previously (25, 26). Briefly, Cells were seeded in 6-well plates (10000 cells/well). After 24 h, they were treated with DCF-DA without (control) or with 10 μ M of different retinoids and with a mixture of SHetA2 and BHA. The cells were maintained at 37°C, and the fluorescence (excitation at 485 nm, emission at 538 nm) was measured at 30-min intervals. Three wells were used for each control or treatment analysis, and the mean \pm SD was determined.

Assay for Detection of MPT. Induction of MPT was evaluated as described previously (27). Briefly, after treatment with different agents, both the floating and attached UMSCC38 cells were collected by trypsinization, and then were incubated with 50 nM DiOC₆ for 15 min at 37°C. A positive control for transmembrane potential loss was obtained by incubation with the uncoupler carbonylcyanide *m*-chlorophenylhydrazone (50 μ M), a protonophore, which disrupts transmembrane potential. The cells were then analyzed using a cytofluorimeter (FacsCaliber, excitation at 488 nm, emission at 552 nm). At least 10,000 events were collected per sample. The suppression of transmembrane potential is represented as a shift of the fluorescence peak to lower levels. The percentage of suppression = $(Y - X)/Y \times 100$, where *X* and *Y* correspond to the observed percentage of MPT in untreated (*Y*) and SHetA2-treated (*X*) samples, respectively. The percentage of cells in the lower fluorescence category was plotted in graphs.

Assay for Detection of Cytochrome *c* Release from Mitochondria by Western Blotting. Semiconfluent cultures of UMSCC38 cells were treated with 10 μ M different retinoids in 10-cm-diameter plates at 37°C for 24 h. At the end of incubation, medium-containing floating cells and attached cells were harvested by trypsinization. Cell suspensions containing both the floating and the attached cells were subjected to centrifugation at 200 \times *g* for 5 min. After resuspension in 1 ml of buffer I [250 μ M sucrose, 30 μ M Tris, 1 μ M EDTA (pH 7.7)], the cells were transferred to microcentrifuge tubes and were placed on ice. Then the cells were centrifuged in a microcentrifuge at 1,000 \times *g* for 1 min. Thirty μ l of buffer I, supplemented with leupeptin (1 μ g/ml), pepstatin (1 μ g/ml), and aprotinin (1 μ g/ml), were used to suspend the cells. The cells were then disrupted by homogenization on ice in a 0.3-ml Kontes Dounce homogenizer with 15 strokes of B pestle. The homogenate was subjected to centrifugation at 16,000 \times *g* for 1 min, and then the supernatant was collected and subjected to another centrifugation at 16,000 \times *g* for 30 min. The supernatant extract (cytosolic fraction) and the resulting pellets containing mitochondria (mitochondrial fraction) were frozen at -80°C. Samples containing 25 μ g of protein from both fractions were loaded on 12% polyacrylamide gel. After electrophoresis, the proteins were transferred to nitrocellulose membrane (Amersham Life Science, Arlington Heights, IL). After inhibiting nonspecific binding sites with 5% (w/v) skim milk, the membrane was incubated with affinity-purified anti-cytochrome *c* antibody 7H8.22C12 (PharMingen, San Diego, CA) diluted 1:1,000 in 1% (w/v) dried milk in 0.2% (v/v) Tween 20 containing PBS (PBST) for 1 h at room temperature. The membrane was then washed three times in PBST and incubated with rabbit antimouse IgG-horseradish peroxidase conjugate (DAKO, Carpinteria, CA) and was diluted 1:2000 in 1% (w/v) dried milk in PBST for 1 h at room temperature. The membrane was then washed four times with PBST, stained with enhanced chemiluminescence reagents from Amersham according to the supplier's instructions, dried, and exposed briefly to X-ray film. The percentage of cytochrome *c* content was calculated by using the equation: % cytochrome *c* content = $[A/(A + B)] \times 100$, where *A* and *B* represent the relative density of Western blotting protein bands of the cytosolic and pellet fractions, respectively.

Assay for Caspase-3-like Protease. Caspase-3-like protease activity was measured by a modification of the method described previously (26). Briefly,

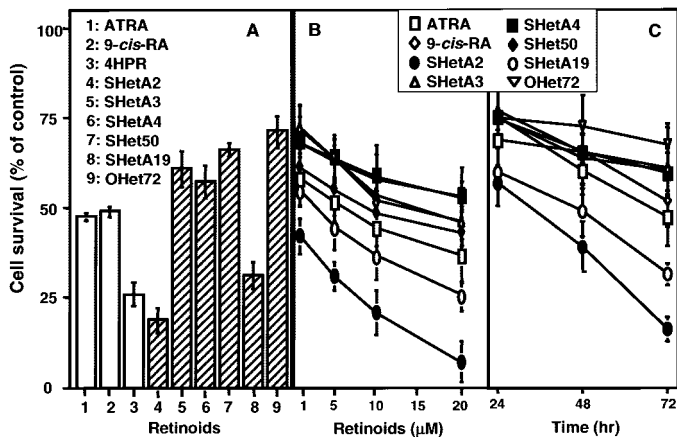


Fig. 2. Hets inhibit survival of HNSCC cells in a dose- and time-dependent manner. A, cells were seeded at a density of 3000 cells/well in 96-well tissue culture plates. After 24 h, cells were treated with 10 μM retinoids. After 3 days, cell numbers were estimated by using the SRB assay. B, cells were treated with different concentrations of retinoids for 3 days. C, cells were treated with each of nine different retinoids (at 10 μM) for 1, 2, and 3 days. Each assay was performed in triplicate, and the results were calculated as the mean ± SE, as described in "Materials and Methods." All eight of the retinoids have been analyzed in both B and C.

UMSCC38 were treated with Hets for 6, 12, 18, and 24 h at 37°C. At the end of each incubation, floating and attached cells were harvested. The cells were centrifuged at 1000 × g for 1 min. The pelleted cells were suspended in 1 ml of lysis buffer [1 mM DTT, 0.125 mM EDTA, 5% glycerol, 1 mM phenylmethylsulfonylfluoride, 1 μg/ml leupeptin, 1 μg/ml pepstatin, 1 μg/ml aprotinin, 1% Triton X-100 in 12.5 mM Tris-HCl buffer (pH 7.0)] at 4°C for 15 min. After centrifugation at 1000 × g for 15 min, cell lysates were diluted with the reaction buffer [1 mM DTT, 0.5 mM EDTA, 20% glycerol in 50 mM Tris-HCl buffer (pH 7.0)] and were incubated at 37°C in the presence of 30 μM of the caspase-3 substrate (acetyl-Asp-Glu-Val-Asp-aminomethylcoumarin). The product was measured at 2-min intervals at 460 nm after excitation at 360 nm using Fluoroskan II. Protein concentration was measured by a dye-binding assay using the Bio-Rad Protein Assay reagents (Bio-Rad Laboratories, Hercules, CA).

Detection of Caspase-3 Activation by Western Blotting. Cytosolic extracts, prepared as above and containing 25 μg protein, were subjected to electrophoresis using 12% polyacrylamide slab gels. The proteins were transferred electrophoretically to polyvinylidene fluoride membrane. The nonspecific binding sites on the membrane were first blocked with 5% (w/v) dried skim milk in PBST. After three washes with PBST, the membrane was incubated with affinity-purified anti-caspase-3 antibody (BD Transduction Laboratories, Lexington, KY) diluted 1:1000 in 1% (w/v) dried skim milk in PBST for 1 h at room temperature. The rest of the procedure was the same as that described above for cytochrome *c* detection.

RESULTS

Differential Effects of Hets on the Survival of UMSCC38 Cells.

We have chosen to use the HNSCC cell line UMSCC38 to explore the mechanism of action of Hets because these cells have been found to be sensitive to some Hets in a xenograft model in nude mice (21). Initially, we examined the effects of treating the cells for 72 h with six different Hets and three retinoids at a concentration of 10 μM (Figs. 1 and 2A). Among the six Hets examined, two (SHetA2 and SHetA19) were found to be more potent than the natural RAs (ATRA and 9-*cis*-RA) in decreasing the survival of UMSCC38 cells, whereas the other four were less potent. SHetA2 was as effective as the potent pro-apoptotic retinoid 4HPR (Fig. 2A). The effects of these retinoids on cell survival were dose dependent and time dependent (Fig. 2, B and C). Decreased cell survival was noticed after 72 h of treatment with concentrations as low as 1 μM for SHetA2 and SHetA19. These

two Hets were also effective after shorter treatment (e.g., 24–48 h; Fig. 2C).

Induction of Apoptosis in UMSCC38 Cells by SHetA2. Apoptosis was determined after treatment with SHetA2 by the TUNEL assay as shown in Fig. 3A. Whereas ATRA induced apoptosis in <10% of the cells after a 72 h-treatment (Fig. 3A), SHetA2 induced apoptosis in 47.5% of the cells after a 24 h-treatment, 72.7% after 48-h treatment, and almost 100% of the total cell population after a 72-h treatment (Fig. 3, A and B). Observations under the microscope revealed that the UMSCC38 cells did not detach even after 72 h of exposure to SHetA2, and they appeared to be intact and did not fragment into apoptotic bodies. Using another apoptosis detection method, the Annexin V binding assay, we confirmed the ability of SHetA2 to induce apoptosis (Fig. 3, C and D). 4HPR (10 μM) induced 12.6% of necrosis and 14.1% of late stage of apoptosis after a 24-h treatment, whereas ATRA was considerably less effective (Fig. 3, C and D). In contrast, SHetA2 induced early-stage apoptosis (8.6%) and late-stage apoptosis (33.8%), but not necrosis (2.9%) after a 24-h treatment (Fig. 3C). Among other Hets, SHetA19 was also effective in inducing both early and late stage of apoptosis whereas the other four Hets were ineffective (Fig. 3C).

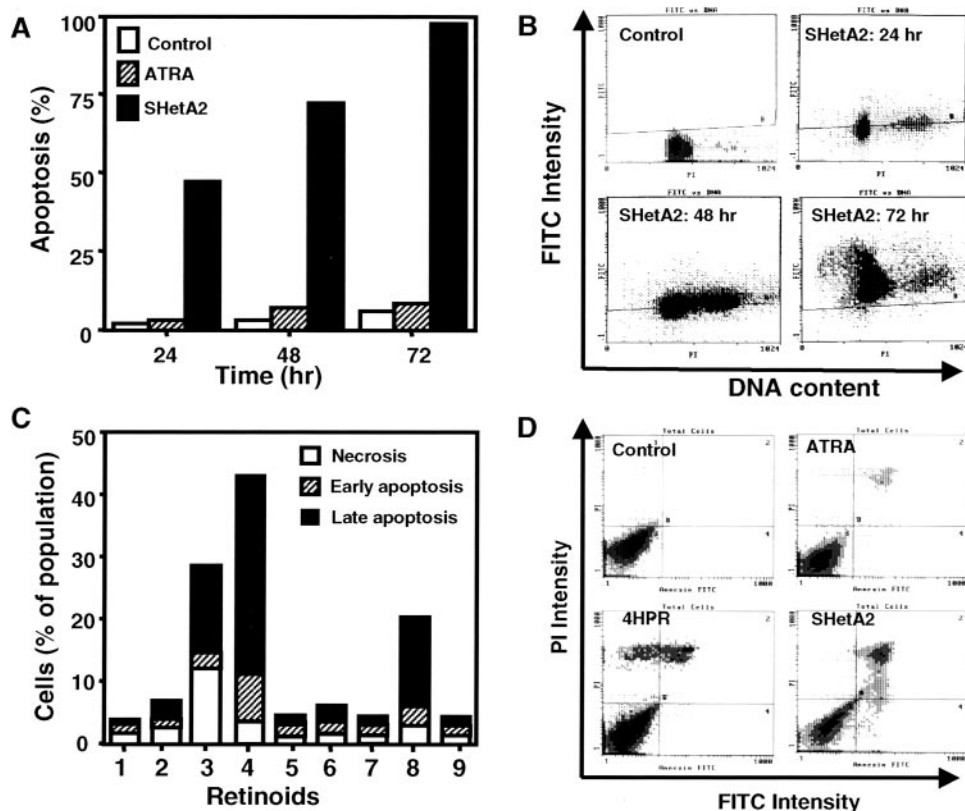
The proapoptotic effect of SHetA2 was not restricted to UMSCC38, as indicated by our finding that seven other HNSCCs were sensitive to treatment with 10 μM SHetA2 (Fig. 4, A and B). SHetA2 was more potent than ATRA in the induction of apoptosis in eight HNSCC cell lines (Fig. 4B).

Apoptosis Induced by SHetA2 Is Independent of Retinoid Receptor-mediated Pathway. The Hets used in this study included four that exhibited no receptor activation capability, one that was specific for activating RXRs, and one that was specific for both RARs and RXRs (Fig. 1). SHetA2 did not transactivate any of the retinoid receptors at concentrations up to 10 μM (Fig. 1). Indeed, neither the pan-RAR-specific antagonist AGN193109 (40 μM) nor the pan-RXR-specific antagonist LG100754 (20 μM) blocked apoptosis induced by SHetA2 (Fig. 4C). Thus, we concluded that apoptosis induced by SHetA2 is independent of activation of RARs or RXRs in the UMSCC38 cells.

UMSCC38 Cells Accumulate in the S and G₂-M Phases of the Cell Cycle after Treatment with SHetA2. Examination of cell cycle distributions in UMSCC38 cells treated with 10 μM SHetA2 revealed that cells were shifted from the G₁ to the S and G₂-M phases after 24 and 48 h compared with DMSO-treated control cells (Fig. 5). In 48-hr treated cultures, the increase in G₂-M was twice as high as at 24 h, mostly because of a further decrease in cells in G₁. We did not observe the accumulation of cells in a sub-G₁ compartment expected from apoptotic cells. The reason may be that the cells had undergone DNA fragmentation but did not form apoptotic bodies therefore the majority of the signals recorded by the flow cytometer was of cells in G₁, S phase, or G₂-M, not sub-G₁.

Treatment of UMSCC38 Cells with SHetA2 Increases Generation of ROS, Suppresses Mitochondrial Permeability Transition, and Induces Cytochrome *c* Release from Mitochondria. The ability of retinoids, such as 4HPR, to induce apoptosis independent of receptor activation has been ascribed in part to induction of ROS (14, 25–27). Therefore, we explored whether SHetA2 shares a similar mechanism. SHetA2 increased the generation of intracellular ROS in UMSCC38 cells within 60 min after treatment. A linear and time-dependent increase in the ROS generation rate was observed up to 240 min (Fig. 6A). Under the same conditions, ATRA caused a gradual but small increase in ROS generation, whereas 4HPR induced ROS generation more effectively than SHetA2. The increase of ROS by SHetA2 treatment was inhibited by cotreatment with the antioxidant BHA (Fig. 6A). Furthermore, BHA was able to suppress induction of

Fig. 3. SHetA2 induces apoptosis in UMSCC38 HNSCC cells. *A* and *B*, cells were harvested after 1, 2, and 3 days of treatment with 10 μ M SHetA2 or ATRA. Apoptosis was detected by the TUNEL assay as described in "Materials and Methods." *C* and *D*, cells were harvested after a 1-day treatment with the indicated retinoids (at 10 μ M; numbered as in Fig. 1). Annexin V-binding assay was used to determine phosphatidylserine externalized to the outer leaflet of the cell surface membrane as described in "Materials and Methods."



apoptosis by SHetA2 (Fig. 6B), suggesting that ROS generation was important for apoptosis induction by SHetA2.

Increased levels of ROS can lead to alterations in the mitochondrial membrane potential followed by the release of caspase-activating factors, such as cytochrome *c*. A kinetic analysis of the uptake of the potential sensitive dye DiOC₆ (25) in SHetA2 treated cells, which is indicative of MPT, demonstrated a time-dependent MPT suppression beginning at 6 h after treatment (Fig. 6C). CsA, the reference inhibitor of MPT (28), prevented the suppression of mitochondria depolarization by SHetA2 in UMSCC38 cells (Fig. 6D).

The suppression of MPT by SHetA2 treatment of UMSCC38 cells was accompanied by the release of cytochrome *c* into the cytoplasm (Fig. 6E). This event was blocked by CsA (Fig. 6E). Moreover, the two MPT inhibitors CsA and TFP (27, 29), suppressed induction of apoptosis by SHetA2 treatment (Fig. 6F).

Activation of Caspase-3 by SHetA2 Treatment. To investigate additional downstream steps in the apoptosis pathway induced by SHetA2, we tested the activation of caspase-3 in UMSCC38 cells using both a Western blotting and a fluorescent substrate assay. Caspase-3-like activity was increased efficiently and time dependently after SHetA2 treatment (Fig. 7A). Procaspase 3 level decreased after treatment, indicating its activation, and, indeed, an analysis of caspase-3 activity has shown an increase cleavage of a synthetic substrate (Fig. 7A, bottom panel). The caspase-3 inhibitor, Ac-DEVD-CHO, inhibited SHetA2-induced apoptosis in UMSCC38 cells (Fig. 7B).

DISCUSSION

The majority of retinoids used in clinical trials to date have exhibited dose-limiting side effects (30–32). Therefore, considerable efforts have been invested in the development of synthetic mimics of RA, which exert similar biological effects but exhibit lower toxicity than RA. One group of retinoids prepared for this purpose is the Hets

(33–35). Hets have been defined as retinoids possessing one aromatic ring and at least one heteroatom (*e.g.*, *O*, *S*, *NR*) in the partially saturated ring. A few members of this group exhibited considerable anticancer activity (19–22). Inclusion of the heteroatom in the ring

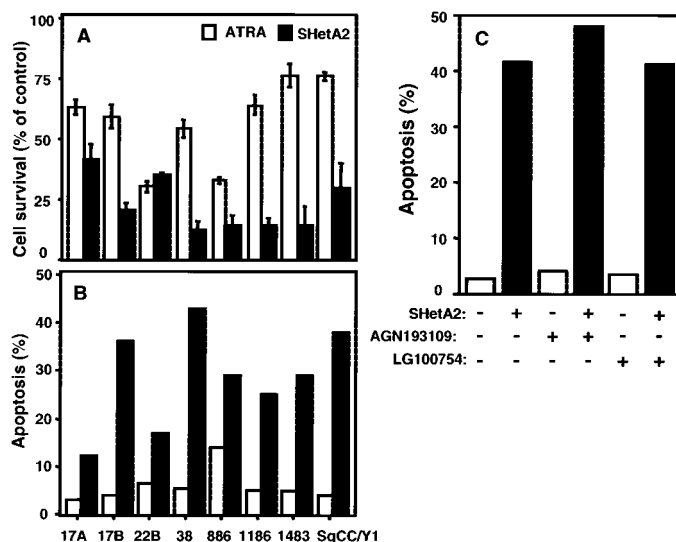


Fig. 4. Effect of SHetA2 on different HNSCC cancer cell lines and effects of the RAR or RXR antagonists on the induction of apoptosis by SHetA2 in UMSCC38 cells. *A* and *B*, effects of SHetA2 on different HNSCC cell lines. After 1 or 3 days of treatment with 10 μ M SHetA2, cells were harvested. Their survival was determined using SRB assay (*A*) and apoptosis was detected using the TUNEL assay (*B*). Cell survival assay was performed in triplicate, and the results were calculated as the mean \pm SE. *C*, cells were treated with SHetA2 alone (10 μ M) or combined with AGN193109 (RAR antagonist; 40 μ M) or LG100754 (RXR antagonist; 20 μ M). Cells were harvested after 24 h and processed for the TUNEL assay as described in "Materials and Methods." The TUNEL apoptosis assays were performed twice independently with similar results.

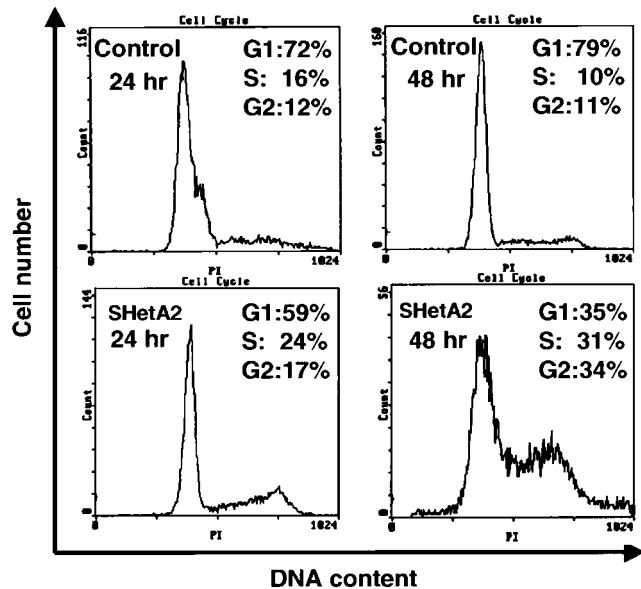


Fig. 5. SHetA2 increases the proportions of cells in the S phase and G₂-M phase of the cell cycle in UMSSC38 cells. Cells were grown with or without 10 μ M SHetA2. After 24 or 48 h, cells were harvested and analyzed using a flow cytometer for DNA contents distribution after propidium iodide staining as described in "Materials and Methods." Results represent two independent experiments. Cells with sub-G₁ DNA content were excluded from analysis by gating to obtain cell cycle distribution of cells without extensive DNA degradation.

has been shown to decrease the toxicity 100-fold in an animal model (19).

Zacheis *et al.* (21) demonstrated that selected Hets inhibit cell proliferation and suppress tumor growth in a xenograft model of HNSCC UMSSC38 cells in nude mice, with no significant toxic effects. SHetA2 did not induce apoptosis in normal ovarian and endometrial cells *in vitro* and exhibited no toxicity to normal tissues *in vivo* in an animal model in which tumor inhibition was clearly observed.⁴

The active Hets exhibited specificity for both RAR and RXR or for RXR only and also suppressed the activity of the activator protein 1 (AP-1) transcription factor. Although the effects of the Hets on apoptosis had not been investigated, the marked regression of established tumors *in vivo* (21) suggested that apoptosis could account for some of the antitumor effects. Recent studies have demonstrated that certain Hets can decrease the growth fraction of ovarian carcinoma cells in organotypic cultures by inducing differentiation or apoptosis (22). Moreover, some Hets were found to induce apoptosis in ATRA-resistant HL60 myeloid leukemia cells (33). However, the mechanism(s) by which Hets induce apoptosis has remained unexplored.

In the present study, we have partially elucidated for the first time some aspects of the mechanisms by which a potent proapoptotic Het, SHetA2, induces apoptosis. Initially, we compared the activities of six Hets with those of the natural ATRA and 9-*cis*-RA and the synthetic 4HPR and found that SHetA2 was the most potent among all of these retinoids in decreasing the survival of UMSSC38 cells by 50% when cells were exposed to even 1 μ M for 72 h. This effect was found to be the result of apoptosis induction. Therefore, subsequent studies were focused on the mechanism of action of this Het. Because the UMSSC38 cells were found to be the most sensitive to SHetA2 among eight different HNSCC cell lines and had also shown sensitivity to Hets *in vivo* (21), we chose these cells for additional studies on the SHetA2 mechanism of apoptosis induction. The apoptosis was confirmed by two independent assays, the TUNEL assay and the Annexin V assay. The latter assay demonstrated also that SHetA2 was

more potent than 4HPR, a potent proapoptotic retinoid (36, 37), in inducing apoptosis in the UMSSC38 cells. The exposure of these cells to SHetA2 also altered the cell cycle distribution such that the proportion of cells in the G₁ phase decreased and that in the S and G₂-M phases increased. There are several examples in the literature of agents that can cause cells to accumulate in G₂-M and induce apoptosis. Such agents include CD437 (38), vinorelbine (39), and arsenic trioxide (40).

SHetA2 does not activate nuclear retinoid receptors (Fig. 1). We excluded a role for nuclear retinoid receptors in the mechanism of apoptosis induction by SHetA2 in UMSSC 38 cells by demonstrating

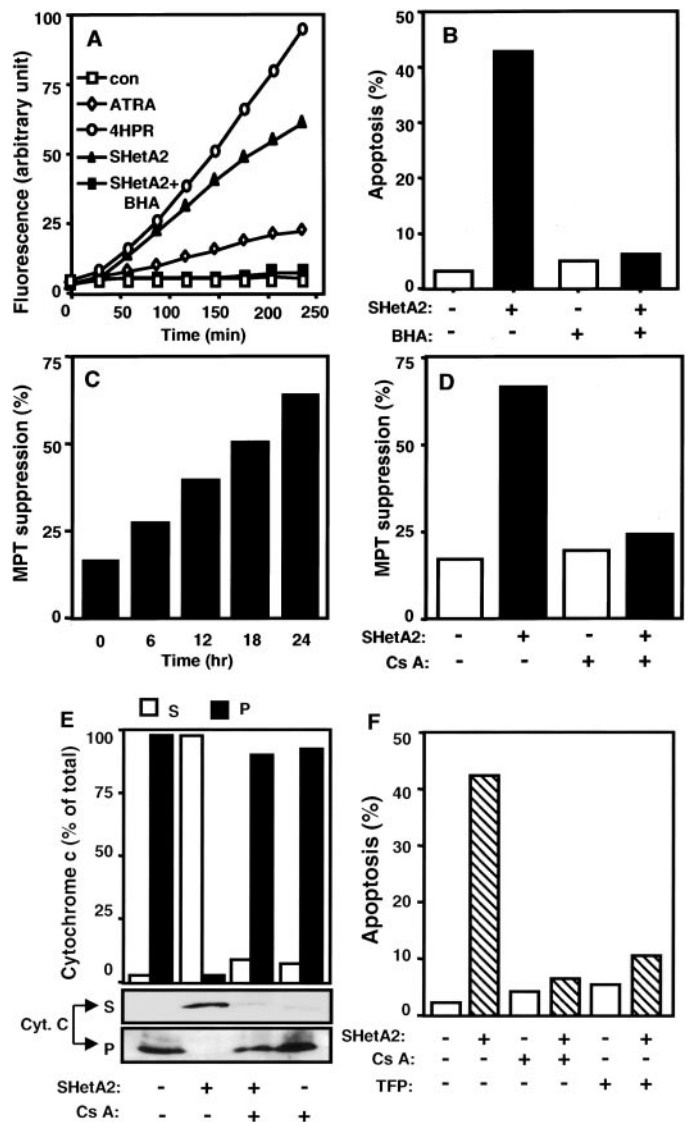


Fig. 6. Effects of SHetA2 on ROS generation, MPT suppression, and cytochrome *c* release in UMSSC38 cells. **A**, cells were treated with the indicated retinoids (at 10 μ M) and with a mixture of SHetA2 (10 μ M) and BHA (50 μ M) in the absence or presence of DCF-DA. The fluorescence of the dichlorofluorescein generated because of the formation of ROS was measured for 240 min (at 30-min intervals); *con*, control. **B**, cells were treated with control medium or with SHetA2 (10 μ M), BHA (50 μ M), or both. After 24 h, cells were harvested, and apoptosis was detected by the TUNEL assay. **C**, cells were treated with 10 μ M SHetA2 for different periods (up to 24 h); then cells were incubated with 50 nM DiOC₆ and analyzed for fluorescence emission representing suppression of MPT as described in "Materials and Methods." **D**, the MPT inhibitor CsA (2 μ M) and the retinoid SHetA2 (10 μ M) were added concurrently or individually to UMSSC38 cells and MPT suppression was determined. **E** and **F**, cells were cultured in the presence of 10 μ M SHetA2 and 2 μ M MPT inhibitor CsA or TFP. After 24 h, cells were harvested and analyzed for: **E**, cytochrome *c* release by Western blotting; and **F**, apoptosis by the TUNEL assay as described in "Materials and Methods."

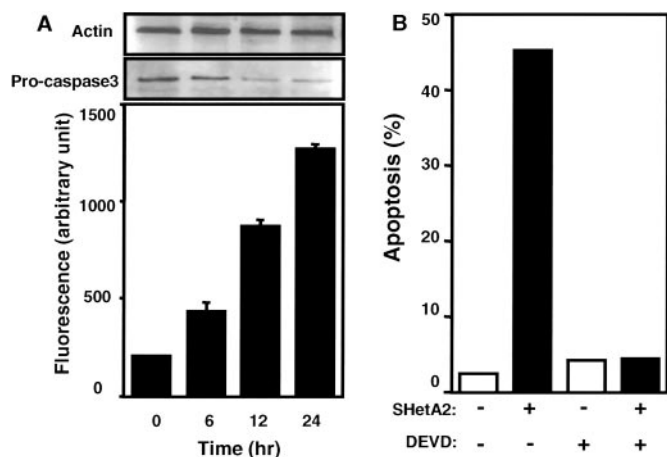


Fig. 7 Activation of caspase-3 and its role in apoptosis induction by SHetA2 in UMSCC38 cells. *A*, cells were treated with SHetA2 for the indicated times, and cells were harvested and analyzed for procaspase-3 level of activity and caspase-3-like activity, as described in "Materials and Methods." The results were calculated as the mean \pm SE of three assays. *B*, cells were treated with 20 μ M caspase-3 inhibitor (Ac-DEVE-CHO) and 10 μ M SHetA2, individually or in combination, as well as with control medium. After 24 h, cells were harvested, and apoptosis was detected by the TUNEL assay.

that the pan-RAR receptor antagonist AGN193109 and the RXR antagonist LG100754 did not affect the ability of SHetA2 to kill cells. It is noteworthy that a previous study has shown that some Hets can inhibit growth of skin cell lines independently of apoptosis via a RAR β -dependent mechanism (20). The ability to induce apoptosis of head and neck cancer cells independently of receptor activation offers promise for the potential of SHetA2 to exhibit reduced toxicity/teratogenicity desired for optimal use in secondary chemoprevention strategies. In previous studies, we and others have shown that the potent apoptosis-inducing retinoid 4HPR triggers apoptosis by increasing the production of ROS in mitochondria (25, 27, 37, 41). In the present study, we have demonstrated that SHetA2 was also an effective ROS inducer, albeit less potently than 4HPR but more effectively than ATRA. The increase in ROS as well as apoptosis could be blocked by the antioxidant BHA, indicating that SHetA2-induced ROS generation is essential for apoptosis as shown for 4HPR (14, 27), as well as for various agents including tumor necrosis factor- α , transforming growth factor- β 1, anti-Fas antibodies, and several chemotherapeutic agents as well as radiation (42–46). Besides increasing ROS, SHetA2 also disrupted MPTP, and this effect was blocked by CsA, which binds to Cyp-M, a cyclophilin-family protein associated with the MPTP, causing it to dissociate from the pore complex (47, 48). This reaction is believed to increase the probability of inhibiting pore flicker and lowers the binding affinity for calcium (49) and inhibits MPTP opening (50). SHetA2-induced opening of the MPTP causes release of cytochrome *c* into the cytoplasm presumably as a consequence of mitochondria swelling and outer membrane rupture (51, 52). The roles of ROS, MPTP, and cytochrome *c* in the mechanisms of SHetA2-induced apoptosis are supported by the finding that not only CsA but also another MPTP inhibitor, TFP-suppressed SHetA2 induced apoptosis.

The release of cytochrome *c* from the mitochondria and its interaction with cytosolic factors including Apaf-1 and dATP can activate caspase-9 and then caspase-3 (52–54). Indeed, we found that SHetA2 treatment of UMSCC38 cells resulted in activation of caspase-3 and that the caspase-3 inhibitor Ac-DEVD-CHO was able to inhibit SHetA2-induced apoptosis.

In conclusion, our results demonstrate that SHetA2 is a potent receptor-independent inducer of apoptosis and point to the mitochondria as the major mediator of this effect at least in UMSCC38 cells.

Additional studies on the potential of SHetA2 for chemoprevention and therapy of ATRA-resistant cancers are warranted based on these findings and the low toxicity of SHetA2.

ACKNOWLEDGMENTS

We thank Drs. Bollag, Chandraratna, and Heyman for some of the retinoids and Drs. Carey, Reiss, and Sacks for the HNSCC cell lines.

REFERENCES

- Moon, R. C., Mehta, R. G., and Rao, K. J. V. N. Retinoids and cancer in experimental animals. *In*: H. M. Sporn, A. B. Roberts, and D. S. Goodman (eds.), *The Retinoids*, pp. 573–595. New York: Raven Press, 1994.
- Hong, W. K., and Itri, L. M. Retinoids and human cancer. *In*: H. M. Sporn, A. B. Roberts, and D. S. Goodman (eds.), *The Retinoids*, pp. 597–658. New York: Raven Press, 1994.
- Lotan, R. Retinoids in cancer chemoprevention. *FASEB J.*, 10: 1031–1039, 1996.
- Evans, T. R. J., and Kaye, S. Retinoids: present role and future potential. *Br. J. Cancer*, 80: 1–8, 1999.
- Gudas, L. J., Sporn, M. B., and Roberts, A. B. The Cellular biology and biochemistry of the retinoids. *In*: H. M. Sporn, A. B. Roberts, and D. S. Goodman (eds.), *The Retinoids*, pp. 443–520. New York: Raven Press, 1994.
- Gottardis, M. M., Lamph, W. W., Shalinsky, D. R., Wellstein, A., and Heyman, R. A. The efficacy of 9-*cis*-retinoic acid in experimental models of cancer. *Breast Cancer Res. Treat.*, 38: 85–96, 1996.
- Shalinsky, D. R., Bischoff, E. D., Lamph, W. W., Zhang, L., Boehm, M. F., Davies, P. J., Nadzan, A. M., and Heyman, R. A. A novel retinoic acid receptor-selective retinoid, ALRT1550, has potent antitumor activity against human oral squamous carcinoma xenografts in nude mice. *Cancer Res.*, 57: 162–168, 1997.
- Bischoff, E. D., Gottardis, M. M., Moon, T. E., Heyman, R. A., and Lamph, W. W. Beyond tamoxifen: the retinoid X receptor-selective ligand LGD1069 (TARGRETIN) causes complete regression of mammary carcinoma. *Cancer Res.*, 58: 479–484, 1998.
- Shalinsky, D. R., Bischoff, E. D., Gregory, M. L., Lamph, W. W., Heyman, R. A., Hayes, J. S., Thomazy, V., and Davies, P. J. Enhanced antitumor efficacy of cisplatin in combination with ALRT1057 (9-*cis* retinoic acid) in human oral squamous carcinoma xenografts in nude mice. *Clin. Cancer Res.*, 3: 511–520, 1996.
- Lotan, R. Suppression of squamous cell carcinoma growth and differentiation by retinoids. *Cancer Res.*, 54 (Suppl.): 1987s–1990s, 1994.
- Oridate, N., Lotan, R., and Lotan, D. Reconstituted basement membrane (Matrigel): a useful semisolid medium for growth of tumor cell colonies. *In Vitro Cell Dev. Biol. Anim.*, 4: 192–193, 1994.
- Lotan, R. Squamous cell differentiation markers in normal, premalignant, and malignant epithelium: effects of retinoids. *J. Cell. Biochem. Suppl.*, 17: 167–174, 1993.
- Sun, S.-Y., Yue, P., Mao, L., Dawson, M. I., Shroot, B., Lamph, W. W., Heyman, R. A., Chandraratna, R. A. S., Shudo, K., Hong, W. K., and Lotan, R. Identification of receptor-selective retinoids that are potent inhibitors of the growth of human head and neck squamous cell carcinoma cells. *Clin. Cancer Res.*, 6: 1563–1573, 2000.
- Sun, S.-Y., Li, W., Yue, P., Hong, W. K., and Lotan, R. Mediation of *N*-(4-hydroxyphenyl) retinamide-induced apoptosis in human cancer cells by different mechanisms. *Cancer Res.*, 59: 2493–2498, 1999.
- Mariani, L., Formelli, F., De Palo, G., Manzari, A., Camerini, T., Campa, T., Di Mauro, M. G., Crippa, A., Delle Grottaglie, M., Del Vecchio, M., Marubini, E., Costa, A., and Veronesi, U. Chemoprevention of breast cancer with fenretinide (4-HPR): study of long-term visual and ophthalmologic tolerability. *Tumorigenesis*, 82: 444–449, 1996.
- Benbrook, D. M. Refining retinoids with heteroatoms. *Minirev. Med. Chem.*, 2: 271–277, 2002.
- Collins, M. D., and Bao, G. E. Teratology of retinoids. *Annu. Rev. Pharmacol. Toxicol.*, 39: 399–430, 1999.
- Elmazar, M. M., Ruhl, R., and Nau, H. Synergistic teratogenic effects induced by retinoids in mice by coadministration of a RAR α - or RAR γ -selective agonist with a RXR-selective agonist. *Toxicol. Appl. Pharmacol.*, 170: 2–9, 2001.
- Benbrook, D. M., Madler, M. M., Spruce, L. W., Birkbichler, P. J., Nelson, E. C., Subramanian, S., Weerasekare, G. M., Gale, J. B., Patterson M. K. Jr., Wang, B., Wang, W., Lu, S., Rowland, T. C., DiSivestro, P., Lindamood, C., III, Hill, D. L., and Berlin, K. D. Biologically active heteroatom retinoids exhibiting anticancer activity and decreased toxicity. *J. Med. Chem.*, 40: 3567–3583, 1997.
- Dhar, A., Liu, S., Klucik, J., Berlin, K. D., Madler, M. M., Lu, S., Ivey, R. T., Zacheis, D., Brown, C. W., Nelson, E. C., Birkbichler, P. J., and Benbrook, D. M. Synthesis, structure-activity relationships, and RAR γ -ligand interactions of nitrogen heteroatom retinoids. *J. Med. Chem.*, 42: 3602–3614, 1999.
- Zacheis, D., Dhar, A., Lu, S., Madler, M. M., Klucik, J., Brown, C. W., Liu, S., Clement, F., Subramanian, S., Weerasekare, G. M., Berlin, K. D., Gold, M. A., Houck, J. R., Jr., Fountain, K. R., and Benbrook, D. M. Heteroatom retinoids inhibit head and neck cancer cell lines *in vitro* and *in vivo* through both RAR and RXR retinoic acid receptors. *J. Med. Chem.*, 42: 4434–4445, 1999.
- Guruswamy, S., Lightfoot, S., Gold, M. A., Hassan, R., Berlin, K. D., Ivey, R. T., and Benbrook, D. M. Effects of retinoids on cancerous phenotype and apoptosis in organotypic cultures of ovarian carcinoma. *J. Natl. Cancer Inst. (Bethesda)*, 93: 516–525, 2001.

23. Lala, D. S., Mukherjee, R., Schulman, I. G., Koch, S. S., Dardashti, L. J., Nadzan, A. M., Croston, G. E., Evans, R. M., and Heyman, R. A. Activation of specific RXR heterodimers by an antagonist of RXR homodimers. *Nature (Lond.)*, *383*: 450–453, 1996.
24. Agarwal, C., Chandraratna, R. A., Johnson, A. T., Rorke, E. A., and Eckert, R. L. AGN193109 is a highly effective antagonist of retinoid action in human ectocervical epithelial cells. *J. Biol. Chem.*, *271*: 12209–12212, 1996.
25. Oridate, N., Suzuki, S., Higuchi, M., Mitchell, M. F., Hong, W. K., and Lotan, R. Involvement of ROS in *N*-(4-hydroxyphenyl) retinamide-induced apoptosis in cervical carcinoma cells. *J. Natl. Cancer Inst. (Bethesda)*, *89*: 1191–1198, 1997.
26. Higuchi, M., Honda, T., Proske, R. J., and Yeh, E. T. Regulation of ROS-induced apoptosis and necrosis by caspase 3-like proteases. *Oncogene*, *17*: 2753–2760, 1998.
27. Suzuki, S., Higuchi, M., Proske, R. J., Oridate, N., Hong, W. K., and Lotan, R. Implication of mitochondria-derived ROS, cytochrome *c* and caspase-3 in *N*-(4-hydroxyphenyl) retinamide-induced apoptosis in cervical carcinoma cells. *Oncogene*, *18*: 6380–6387, 1999.
28. Marchetti, P., Zamzami, N., Joseph, B., Schraen-Maschke, S., Mereau-Richard, C., Costantini, P., Metivier, D., Susin, S. A., Kroemer, G., and Formstecher, P. The novel retinoid 6-[3-(1-adamantyl)-4-hydroxyphenyl]-2-naphthalene carboxylic acid can trigger apoptosis through a mitochondrial pathway independent of the nucleus. *Cancer Res.*, *59*: 6257–6266, 1999.
29. Hoyt, K. R., Sharma, T. A., and Reynolds, I. J. Trifluoperazine and dibucaine-induced inhibition of glutamate-induced mitochondrial depolarization in rat cultured forebrain neurones. *Br. J. Pharmacol.*, *122*: 803–808, 1997.
30. Park, S. H., Gray, W. C., Hernandez, I., Jacobs, M., Ord, R. A., Sutharalingam, M., Smith, R. G., Van Echo, D. A., Wu, S., and Conley, B. A. Phase I trial of all-*trans*-retinoic acid in patients with treated head and neck squamous carcinoma. *Clin. Cancer Res.*, *6*: 847–854, 2000.
31. Soignet, S. L., Miller, V. A., Pfister, D. G., Bienvenu, B. J., Ho, R., Parker, B. A., Amyotte, S. A., Cato, A., III, and Warrell, R. P., Jr. Initial clinical trial of a high-affinity retinoic acid receptor ligand (LGD1550). *Clin. Cancer Res.*, *6*: 1731–1735, 2000.
32. Younes, A., Cristofanilli, M., McLaughlin, P., Hagemeister, F. B., Weber, D., Mesina, O., and Cabanillas, F. Experience with 9-*cis* retinoic acid in patients with relapsed and refractory non-Hodgkin's lymphoma. *Leuk. Lymphoma*, *40*: 79–85, 2000.
33. Spruce, L. W., Gale, J. B., Berlin, K. D., Verma, A. K., Breitman, T. R., Ji, X. H., and van der Helm, D. Novel heteroarotinoids: synthesis and biological activity. *J. Med. Chem.*, *34*: 430–439, 1991.
34. Benbrook, D. M., Subramanian, S., Gale, J. B., Liu, S., Brown, C. W., Boehm, M. F., and Berlin, K. D. Synthesis and characterization of heteroarotinoids demonstrate structure specificity relationships. *J. Med. Chem.*, *41*: 3753–3757, 1998.
35. Simoni, D., Roberti, M., Invidiata, F. P., Rondanin, R., Baruchello, R., Malagutti, C., Mazzali, A., Rossi, M., Grimaudo, S., Capon, F., Dusonchet, L., Meli, M., Raimondi, M. V., Landino, M., D'Alessandro, N., Tolomeo, M., Arindam, D., Lu, S., and Benbrook, D. M. Heterocycle-containing retinoids. Discovery of a novel isoxazole arotinoid possessing potent apoptotic activity in multidrug and drug-induced apoptosis-resistant cells. *J. Med. Chem.*, *44*: 2308–2318, 2001.
36. Lotan, R. Retinoids and apoptosis: implications for cancer chemoprevention and therapy. *J. Natl. Cancer Inst. (Bethesda)*, *87*: 1655–1657, 1995.
37. Delia, D., Aiello, A., Lombardi, L., Pelicci, P. G., Grignani, F., Grignani, F., Formelli, F., Menard, S., Costa, A., and Veronesi, U. *N*-(4-Hydroxyphenyl)retinamide induces apoptosis of malignant hemopoietic cell lines including those unresponsive to retinoic acid. *Cancer Res.*, *53*: 6036–6041, 1993.
38. Shyu, R. Y., Lin, D. Y., Reichert, U., and Jiang, S. Y. Synthetic retinoid CD437 induces cell-dependent cycle arrest by differential regulation of cell cycle associated proteins. *Anticancer Res.*, *22*: 2757–2764, 2002.
39. Erjala, K., Pulkkinen, J., Kulmala, J., Alanen, K., and Grenman, R. Head and neck squamous cell carcinoma is highly sensitive to vinorelbine *in vitro*. *Anticancer Res.*, *22*: 3135–3142, 2002.
40. Liu, Q., Hilsenbeck, S., and Gazitt, Y. Arsenic trioxide-induced apoptosis in myeloma cells: p53-dependent G₁ or G₂-M cell cycle arrest, activation of caspase 8 or caspase 9 and synergy with APO2/TRAIL. *Blood*, *101*: 4078–4087, 2003.
41. Hail, N., Jr., and Lotan, R. Mitochondrial respiration is uniquely associated with the prooxidant and apoptotic effects of *N*-(4-hydroxyphenyl)retinamide. *J. Biol. Chem.*, *276*: 45614–45621, 2001.
42. Remacle, J., Raes, M., Toussaint, O., Renard, P., and Rao, G. Low levels of ROS as modulators of cell function. *Mutat. Res.*, *316*: 103–122, 1995.
43. Buttke, T. M., and Sandstrom, P. A. Oxidative stress as a mediator of apoptosis. *Immunol. Today*, *15*: 7–10, 1994.
44. Meyer, M., Schreck, R., and Baeuerle, P. A. H₂O₂ and antioxidants have opposite effects on activation of NF- κ B and AP-1 in intact cells: AP-1 as secondary antioxidant-responsive factor. *EMBO J.*, *12*: 2005–2015, 1993.
45. Schulze-Osthoff, K., Beyaert, R., Vandevoorde, V., Haegeman, G., and Fiers, W. Depletion of the mitochondrial electron transport abrogates the cytotoxic and gene-inductive effects of TNF. *EMBO J.*, *12*: 3095–30104, 1993.
46. Ohba, M., Shibamura, M., Kuroki, T., and Nose, K. Production of hydrogen peroxide by transforming growth factor- β 1 and its involvement in induction of egr-1 in mouse osteoblastic cells. *J. Cell. Biol.*, *126*: 1079–1088, 1994.
47. Chinnaiyan, A. M., O'Rourke, K., Lane, B. R., and Dixit, V. M. Interaction of CED-4 with CED-3 and CED-9: a molecular framework for cell death. *Science (Wash. DC)*, *275*: 1122–1126, 1997.
48. Connern, C. P., and Halestrap, A. P. Purification and N-terminal sequencing of peptidyl-prolyl *cis-trans*-isomerase from rat liver mitochondrial matrix reveals the existence of a distinct mitochondrial cyclophilin. *Biochem. J.*, *284*: 381–385, 1992.
49. Crompton, M. The mitochondrial permeability transition pore and its role in cell death. *Biochem. J.*, *341*: 233–249, 1999.
50. Halestrap, A. P., McStay, G. P., and Clarke, S. J. The permeability transition pore complex: another view. *Biochimie*, *84*: 153–166, 2002.
51. Green, D. R., and Reed, J. C. Mitochondria and apoptosis. *Science (Wash. DC)*, *281*: 1309–1312, 1998.
52. Li, P., Nijhawan, D., Budihardjo, I., Srinivasula, S. M., Ahmad, M., Alnemri, E. S., and Wang, X. Cytochrome *c* and dATP-dependent formation of Apaf-1/caspase-9 complex initiates an apoptotic protease cascade. *Cell*, *91*: 479–489, 1997.
53. Zou, H., Henzel, W. J., Liu, X., Lutschg, A., and Wang, X. Apaf-1, a human protein homologous to *C. elegans* CED-4, participates in cytochrome *c*-dependent activation of caspase-3. *Cell*, *90*: 405–413, 1997.
54. Chinnaiyan, A. M., Chaudhary, D., O'Rourke, K., Koonin, E. V., and Dixit, V. M. Role of CED-4 in the activation of CED-3. *Nature (Lond.)*, *388*: 728–729, 1997.